# URANS COMPUTATIONS OF A DTMB 5415

**Jorge Izquierdo (CEHINAV Universidad Politécnica de Madrid, Spain)**
**Leo M. González (CEHINAV Universidad Politécnica de Madrid, Spain)**

## 1. SUMMARY

This paper presents the results of the computations performed in the Canal de Ensayos Hidrodinámicos de ETSI Navales (CEHINAV) for the US Navy Combatant DTMB 5415 [Larsson et al. 2003] at model scale with the URANS free surface commercial solver StarCCM+. In this context we focused on the results required to complete the case 3.1a. In this situation the bare hull ship is fixed in a specified position and sails in still water. These computational results are validated against experimental data [Olivieri et al. 2001] in terms of various global and local quantities.

## 2. INTRODUCTION

The StarCCM+ code is based on a finite volume discretization [Demirdzic et al. 1995, Weiss et al. 1999, Muzaferija et al. 1999]. In the finite volume method the solution domain in divided into a finite number of small control volumes corresponding to the cells of the computational grid. Discrete versions of the integral form of the continuum transport equations, mass and momentum conservation are applied to each control volume. The objective is to obtain a set of linear algebraic equations, with the total number of unknowns in each equation system corresponding to the number of cells in the grid. In the case presented in this paper, the Navier-Stokes equations present a dominant non-linearity and iterative techniques that rely on suitable linearization strategies must be employed [Ferziger et al. 2002].

The turbulence model used in the calculations was the SST (Shear Stress Transport) based on two equation blended k-ω model [Menter 2003]. The use of a blending function, which includes functions of wall distance, also implements the cross diffusion term far from the walls, but not near the walls. This approach effectively blends the k-epsilon model in the far-field with the k-Omega model near the wall. This approach cures the biggest drawback to applying the k-Omega model to practical flow simulations.

The volume of fluid method technique (VOF) is used to model the free-surface flow. The VOF method seems to be one of the most promising for free surface calculations, but it still requires some improvement [Kleefsman, 2005].
The two-phase Unsteady Reynolds Averaged Navier-Stokes (URANS) equations are solved in relative inertial coordinates, where no relative movement is allowed between the grid and the ship [Ghia et al. 1982]. An implicit unsteady Euler predictor-corrector scheme is used for time discretization scheme. The Euler method is not as accurate as the Newmark second order method, so a smaller time step is required to obtain the same accuracy. For a given time step, the Euler method incurs more numerical damping than the second order version for modes which are at a higher frequency than a time-step can resolve. However, our experience was that we found the Euler method more stable and useful for damping out high frequency and small wavelength oscillations. It is important to remark that in stationary cases as the one studied here, the time dependant part of the simulation has a minor role in the final result. Convection term is discretized using a 1st-order upwind scheme and diffusion term using 2nd-order central difference scheme. The Segregated Flow solver controls the solution update according to the SIMPLE algorithm. A segregated flow solver computes the flow equations, one for each velocity components and one for the pressure in a uncoupled manner. The linkage between the momentum and continuity equation is achieved with a predictor-corrector approach. The complete formulation of this algorithm uses a collocated variable arrangement and Rhie-Chow pressure velocity coupling combined with a SIMPLE model. The SIMPLE solver algorithm can be described by the following steps:

1-Solve the discretized momentum equation to create an intermediate velocity $\mathbf{v}^*$.
2-Solve the pressure correction equation to produce cell values of the pressure correction p*. The pressure correction equation is linearized and solved by an algebraic multigrid iterative solver.
3-Update the pressure field $p^{n+1} = p^n + \omega\, p^*$, where ω is a under-relaxation factor for pressure.
4- Correct the cell velocities.

The Message Passing Interface (MPI) library is used in order to handle the domain decomposition, where each decomposed block is mapped to a single processor.
Parallel computation on 3 processors was adopted to reduce the required computational time. The grid is formed by 300k elements for a physical time equivalent to $20L/U_0$. Each simulation took 10 hours of clock time and 30 hours of CPU time.
The platform used in the computations is a PowerEdge cluster 2950 which consist of 4 CPUs/node with 8 cores per node. Each core has 1GB memory.

## 3. GEOMETRY, GRIDS AND BOUNDARY CONDITIONS USED.

Due to the symmetry of the problem, the simulation was carried out using half domain and using the plane Y=0 as the symmetry plane, see figure 1. The domain size in [X,Y, Z] is given by [-1.0-3.0L, 0-2L, -1.5-0.75L], where L is main dimension of the ship.

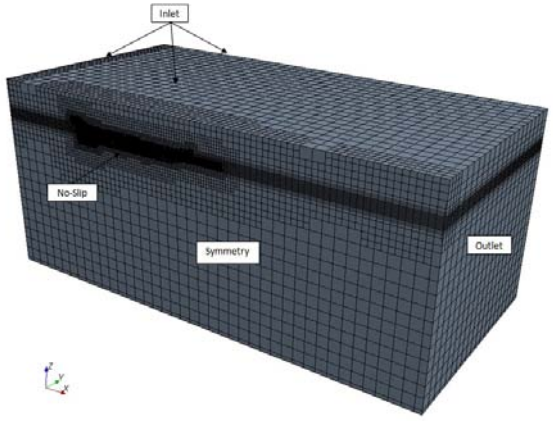


Fig 1. Domain and grid S1 used for the simulation. Boundary conditions are labeled in the corresponding boundary planes.

Three grids have been used for this model. First a coarse grid, mesh S1, of 300k elements was initially used. Later, this initial mesh was systematically refined in order to obtain converged results. Consequently, the first mesh was globally refined with a refinement ratio $r_G$=5/3 obtaining a medium mesh S2 with 1.1 M elements. Finally this second mesh was also refined with a refinement ratio of $r_G$=6/5 giving the finest mesh S3 which is a 2M element grid. The mesh is formed by hexahedral and tetrahedral cells and it also has a prism layer around the hull. In order to capture more accurately the wave formation, the mesh has also been refined around the free surface.

The boundary conditions used in these simulations are the following: the hull has no-slip boundary condition, this means that the velocity is explicitly set to zero and the boundary face static pressure is extrapolated from the adjacent cells using reconstruction gradients. Due to the turbulence model used, a wall treatment has been used in the simulation trying to keep the non dimensional parameter $y^+$>30. A wall treatment in STAR-CCM+ is the set of near wall modeling assumptions for each turbulence model. In figure 2 the $y^+$ has been plotted along the ship hull and we can observe that when the grid size is reduced the value of the non dimensional y+ is kept below the recommended value. The inflow ($X_{min}$) plane has a uniform velocity $U_0$ and the pressure follows an hydrostatic distribution, and for the outflow ($X_{max}$) plane extrapolated velocity and hydrostatic pressure are imposed. As it was written before, a symmetry condition is used for the plane Y=0, this means that the face values of the velocity and pressure is computed by extrapolating the parallel component of velocity in the adjacent cells using reconstruction gradients. For the rest of the planes: Y-max, Z-max and Z-min, inlet velocities $U_0$ are imposed and a zero-gradient boundary condition is used for pressure.

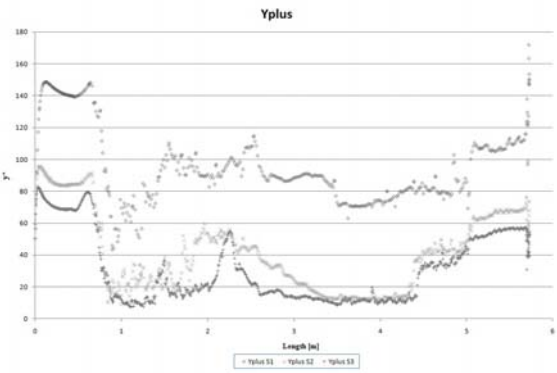


Fig 2. Values of $y^+$ along the ship hull for the three different meshes used.

## 4. SHIP RESISTANCE

During the simulation the ship resistance parameters were calculated and these numbers were used as stopping criteria for the time marching problem. The force on the hull surface is computed as the global action of the viscous shear force and the pressure force. The pressure used in each surface is the result of the face pressure minus the reference pressure. In our case the reference pressure is fixed and equal to the atmospheric pressure. As can be observed in Table 1, the grid refinement affects quantitatively the computation of the resistance parameters. In the case of the coarsest grid S1 the total resistance coefficient $C_T$ has been calculated with an error of less than 1%. The contribution of the viscous and pressure forces to this global resistance is over predicted for the viscous prediction while the pressure contribution is under predicted. In one hand, the viscous case, the coefficient $C_F$ was computed with an error that is less than 2% for all the grids used. On the other hand, the coefficient $C_R$ was computed with an error that is just less than 7% for the coarsest grid S1. The V&V study of these results reveals that the only mesh that verifies that the total error of the drag prediction, 0.55%*D* is less than $U_V$=3.57%*D*, is the coarsest grid S1.

This fact confirms that our prediction is validated with the mesh S1, anyway systematic mesh refinements were performed to improve other computed results as the wave contour elevation.

| Parameters | *EFD* | ITTC | Grid S3 | Grid S2 | Grid S1 |
|---|---|---|---|---|---|
| $C_T \times 10^3$ | **4.23** | | 4.04 | 4.06 | 4.21 |
| $C_F \times 10^3$ | | **2.91** | 2.93 | 2.93 | 2.97 |
| $C_R x 10^3$ | **1.32** | | 1.10 | 1.13 | 1.24 |

Table 1. Summary of the ship resistance prediction for the conditions of the case 3.1.a.

## 5. WAVE PROFILE CALCULATIONS.

When resistance coefficients were finally converged in time the wave profiles has been plotted at different distances from the symmetry plane. In figure 3 the global wave contour elevation can be appreciated when the finest mesh S3 has been used. In figures 4, 5 and 6 we can see different wave cuts computed with meshes S1 and S3 at $y/L_{pp} = 0.082$, 0.172 and 0.301. These plots are compared with the EFD results, see Olivieri et al. 2001 and the agreement is reasonable. Although the predictions are accurate, it is important to remark that the error in the maximums of wave profile grows when the wave cut increases, this fact can be observed in Figure 6 for the peaks at x=1.0 and x=1.2 where the maximums and the minimums of the wave profile are slightly over predicted. In figures 4, 5 and 6 we can observe that the accuracy of the wave cut improves when the finest grid S3 is used.

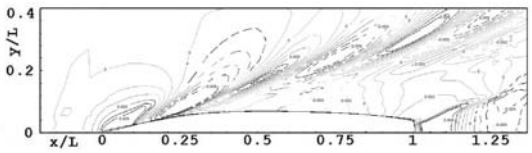


Fig 3. Wave contour elevation .Mesh S3

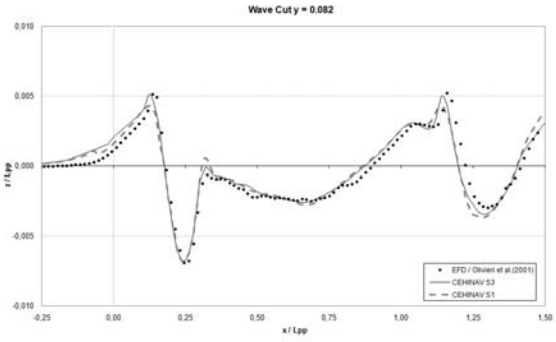


Fig 4. Wave cut, $y/L_{pp} = 0.082$.

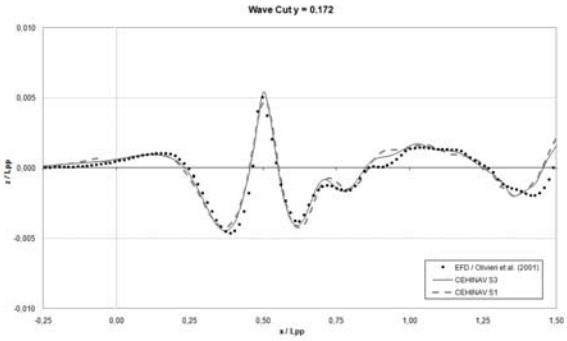


Fig 5. Wave cut, $y/L_{pp} = 0.172$.

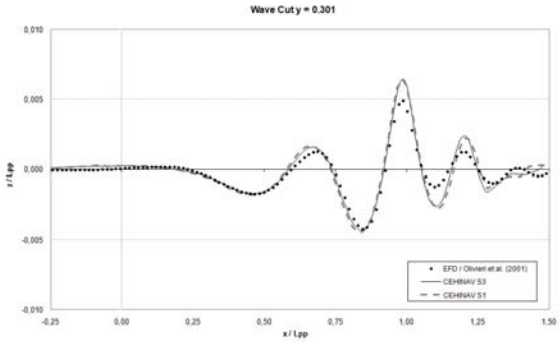


Fig 6. Wave cut, $y/L_{pp} = 0.301$.

## 6. VELOCITY FIELDS

Once the simulation has reached the steady state, the velocity field has been plotted at different planes normal to the X direction. The velocity fields have been plotted in five different normal planes, these planes are set at $X/L_{pp}$ =0.1, 0.2, 0.6, 0.8, 0.935 and 1.1

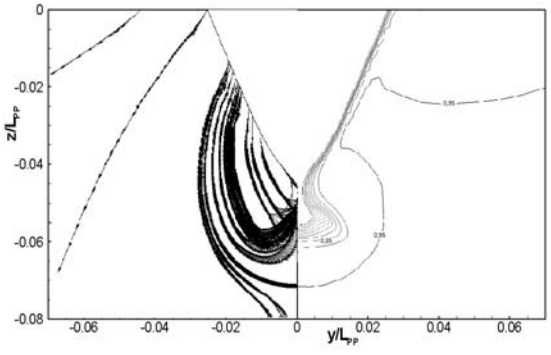


Fig 7. U contour lines (right panel), cross flow streamlines (left panel) at $x/L_{pp} = 0.1$.

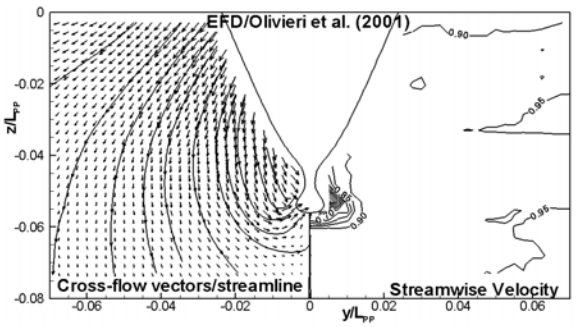


Fig 8. Experimental results at $x/L_{pp}$= 0.1. As before, U contour lines (right panel), cross flow streamlines (left panel).

In the left panel of Figure 7 and 9 the boundary layer attached to the ship hull can be easily appreciated. In Figure 7, the streamlines plotted in the right panel are clearly influenced by the presence of the bulb that divides the flow in two different parts. The first part is formed by the streamlines that start in a hull point and finish far away of the ship and the second part are streamlines that also start in a hull point but keep themselves inside a fluid bubble where the streamlines are finally reattached close to the bulb. This velocity distribution has a remarkable agreement with the one shown in Figure 8 where the reattached streamlines are also present on the right panel.

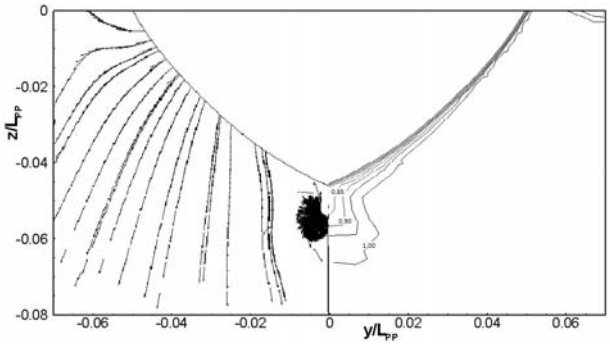


Fig 9. U contour lines (right panel), cross flow streamlines (left panel) at $x/L_{pp}$= 0.2.

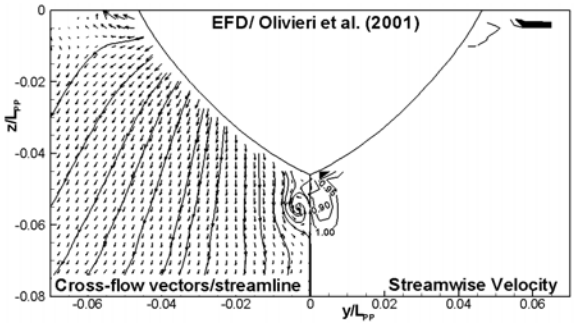


Fig 10. Experimental results at $x/L_{pp}$= 0.2. As before, U contour lines (right panel), cross flow streamlines (left panel)..

In figure 9 the projection of the vortex detached because of the presence of the bulb is clearly appreciated. Most of the streamlines that are plotted on the right panel of Figure 9 just show how the flow feels the section of the boat is increasing towards the X direction. The equivalent experimental result is shown in Figure 10 where the vortex is also present at the bottom of the hull. This situation is clearly changed in Figures 11, 12 and 13, the sections presented in these cases have $x/L_{pp} > 0.5$, this means that the section is decreasing towards the X direction, this changes drastically the direction of the flow.

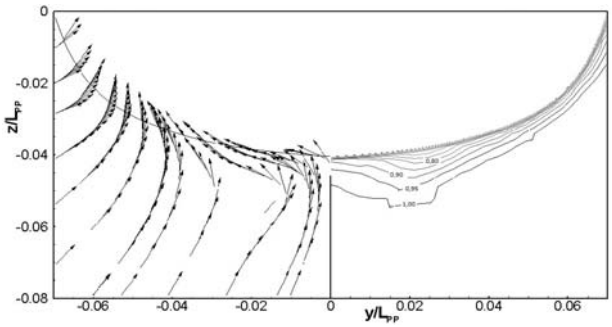


Fig 11. U contour lines (right panel), cross flow streamlines (left panel) at $x/L_{pp}$= 0.6.

In Figures 14 and 15, the section represented is just behind the ship $X/L_{pp}$=1.1, consequently the wake of the flow can be perfectly appreciated. It is important to remark that the central vortex coming out of the wake is well captured by the simulation. In the right panel of Figure 14 the recirculation of the flow is clearly visible. Comparing these results to the ones coming from the experimental study some differences can be noticed. First, the centre of the vortex is set in a slight different position, closer to the central axis in the computational case. Second, the streamlines at the bottom of the Figures 14 seem to follow the behavior of the central vortex, while those streamlines are out of the vortex bubble as can be seen in Figure 15. The consequence of this is that the streamlines of the computational version are more influenced by the presence of the vortex than the ones obtained by the experimental measurements.

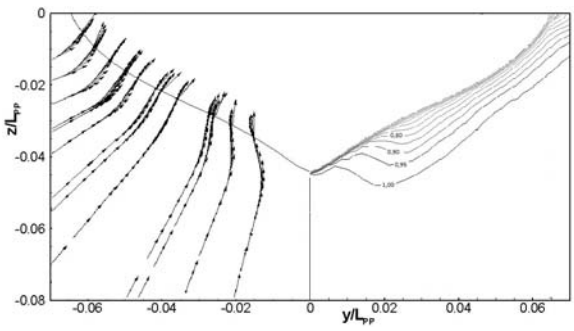


Fig 12. U contour lines (right panel), cross flow streamlines (left panel) at $x/L_{pp}$= 0.8.

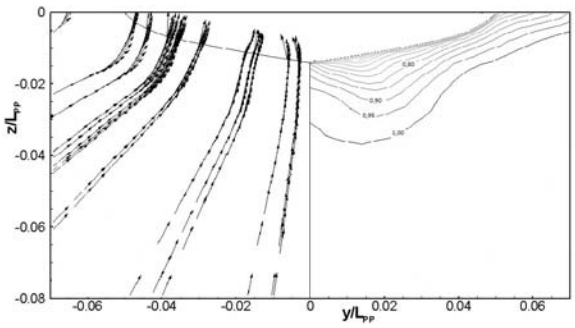

Fig 13. U contour lines (right panel), cross flow streamlines (left panel) at $x/L_{pp}$= 0.935.

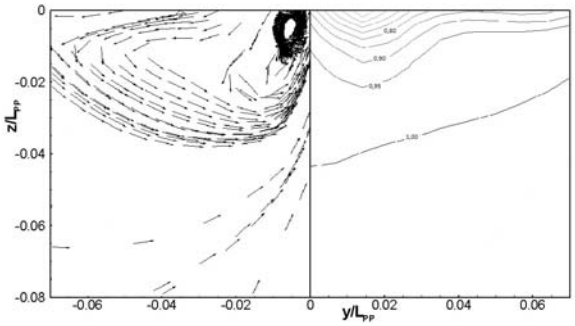

Fig 14. U contour lines (right panel), cross flow streamlines (left panel) at $x/L_{pp}$= 1.1.

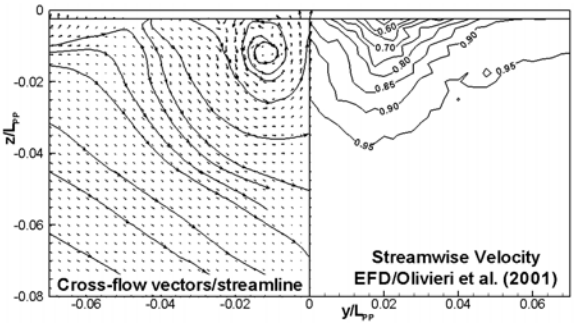


Fig 15. Experimental results at $x/L_{pp}$= 1.1. As before, U contour lines (right panel), cross flow streamlines (left panel).

## 7. CONCLUSION

This paper has presented the results of the required computations for the case 3.1a performed in the CEHINAV for the US Navy Combatant DTMB 5415 at model scale. For this task the URANS equations were solved using the commercial solver StarCCM+. In this case the bare hull ship is fixed in a specified position and sails in still water. The comparison is done in terms of global quantities as resistance coefficients and also comparing wave cuts and velocity fields where local differences could be appreciated. Three different grids have been used for the computations and the V&V test has been used to validate our predictions. The coarsest mesh obtained accurate enough results, but more refined meshes were used to improve the wave cut calculation. The relative error obtained in the ship total resistance with the coarsest grid was less than 1%. The comparison of the wave cuts and velocity fields of the computational results to experimental data given by the organizers of the Workshop presents a remarkable agreement. Consequently, the code Star CCM+ has shown that is a useful tool for the prediction of the fluid quantities in ship hydrodynamics.

## ACKNOWLEDGMENTS

The research has been funded by the Spanish Administration included in the project TRA 2005 – 08866 – C02-01.

## REFERENCES

Larsson, L., Stern, F. and Bertram, V., (2003), "Benchmarking of Computational Fluid Dynamics for Ship Flows: the Gothenburg 2000 Workshop", *Journal of Ship Research*, Volume 47, No 1, March

Ferziger, J.H. and Peric, M., (2002), "*Computational Methods for Fluid Dynamics*", 3rd Ed., Springer Verlag, Berlin, Heidelberg

Van, S.H., Kim, W.J., Yim, G.T., Kim, D.H., and Lee, C.J., (1998b), "Experimental Investigation of the Flow Characteristics Around Practical Hull Forms," Proceedings 3rd Osaka Colloquium on Advanced CFD Applications to Ship Flow and Hull Form Design, Osaka, Japan

Olivieri, A., Pistani. F., Avanaini, A., Stern, F., and Penna, R. (2001), "Towing Tank Experiments of Resistance, Sinkage and Trim, Boundary Layer, Wake, and Free Surface Flow Around a Naval Combatant INSEAN 2340 Model," Iowa Institute of Hydraulic Research, The University of Iowa, IIHR Report No. 421, 56 pp.

K.M.T. Kleefsman, G. Fekken, A.E.P. Veldman, B. Iwanowski, B. Buchner, A Volume-of-Fluid based simulation method for wave impact problems, Journal of Computational Physics, Volume 206, Issue 1, 10 June 2005, Pages 363-393, ISSN 0021-9991, DOI: 10.1016/j.jcp.2004.12.007.

Menter, F.R. "Two-equation eddy-viscosity turbulence models for engineering applications" AIAA-Journal, 32(8), 1994.

Industries Inc., 1993. 460pp.

U. Ghia, K. N. Ghia, C. T. Shin, High-Re solutions for incompressible flow using the Navier-Stokes equations and a multigrid method, Journal of Computational Physics, Volume 48, Issue 3, December 1982, Pages 387-411

Demirdzic, I., Muzaferija, S. “Numerical method for coupled fluid flow, heat transfer and stress analysis using unstructured moving meshes with cells of arbitrary topology”, Comput. Methods Appl. Mech. Engrg., Vol. 125 pp. 235-255 (1995).

Weiss, J., Maruszewski, J.P., Smith, W.A “Implicit solution of preconditioned Navier-Stokes equations using algebraic multigrid”, AIAA J., Vol. 37, pp. 29-36 (1999).

Wilcox D. C..”Turbulence Modelling for CFD”. By DCW

Muzaferija, S., Peric, M. “Computation of free surface flows using interface-tracking and interface-capturing methods”, In O. Mahrenholtz, M. Markiewicz (eds.), Nonlinear Water Wave Interaction, Chap. 2, pp. 59-100, WIT Press, Southampton, 1999.

CD-Adapco “Star-CCM+ User Guide” version 5.02.009, 2010.http://www.cd-adapco.com/products/STAR-CCM_plus/